Lab on a Chip

PAPER

Cite this: *Lab Chip*, 2017, **17**, 2003

Thermal scribing to prototype plastic microfluidic devices, applied to study the formation of neutrophil extracellular traps†

Arvind Chandrasekaran,[a] Nikita Kalashnikov,[a] Roni Rayes,[b] Claire Wang,[b] Jonathan Spicer[b] and Christopher Moraes *[acd]

Innovation in microfluidics-based biological research has been aided by the growing accessibility of versatile microscale fabrication techniques, particularly in rapid prototyping of elastomeric polydimethylsiloxane (PDMS) based devices. However, the use of PDMS presents considerable and often unexpected limitations, particularly in interpreting and validating biological data. To rapidly prototype microfluidic culture systems in conventional plastics commonly used in cell culture, we developed 'thermal scribing', a one-step micromachining technique in which thermoplastics are locally patterned by a heated tip, moving in user-controlled patterns. To demonstrate and study the thermal scribing process, we modified an inexpensive desktop hobby craft cutter with a soldering iron to scribe micropatterns on polystyrene substrates. The thermal scribing technique is useful for creating a variety of channel profiles and geometries, which cannot be readily achieved using other microfabrication approaches. The entire fabrication process, including post-processing operations needed to fabricate devices, can be completed within a few hours without the need for skilled engineering expertise or expensive equipment. We apply this technique to demonstrate that induction of functional neutrophil extracellular traps (NETs) can be significantly enhanced over previous studies, when experiments are conducted in microfluidic channels prototyped in an appropriate material. These results ultimately inform the design of neutrophil culture systems and suggest that the inherent ability of neutrophils to form NETs may have been significantly under-reported.

Received 1st April 2017,
Accepted 11th May 2017

DOI: 10.1039/c7lc00356k

rsc.li/loc

1. Introduction

The capacity for microfluidic systems to handle small sample volumes, with high experimental throughput in a portable and easy-to-prototype format has significantly impacted the fields of tissue engineering,[1] single cell biology,[2] drug discovery,[3,4] synthetic biology,[5] and point-of-care diagnostics.[6] Innovation in these areas has been driven by simple and readily-accessible fabrication technologies, in which engineers and scientists may rapidly prototype, iterate and refine proof-of-concept elastomeric devices that have been uniquely designed to study their system of interest. However, use of these elastomeric polymer systems to construct devices may significantly and unexpectedly impact biological function,[7–9] suggesting the need to rapidly prototype devices in alternative materials more commonly used in biological studies. Here, we present a simple, well-controlled, and readily accessible thermal scribing process to rapidly produce customized microfluidic devices in polystyrene materials, and demonstrate the potential impact of the selected construction material on the production of neutrophil extracellular traps in microfluidic systems.

Although rarely used in commercial-scale applications,[10] polydimethylsiloxane (PDMS) is the *de facto* standard material of choice for microfabricated systems in most academic labs,[11] based on the gas permeability, low toxicity, accessibility and ease of processing of the material to create micron- to millimeter scale features. Though the fabrication technique involved in making the mold for PDMS soft lithography often requires the use of an expensive cleanroom facility, novel alternative techniques are being developed to fabricate microfluidic devices using a xurographer to cut channels directly in PDMS sheets,[12] or create soft lithography master molds in multilayered materials.[13–16] However, PDMS presents significant downstream challenges in interpreting data from biomicrofluidic experiments.[17] For example, elastomeric channels may deform under high pressure flow, altering experimental conditions; and are known to alter surface functionalization properties over time.[18] More broadly, PDMS materials leach oligomers from

[a] *Department of Chemical Engineering, McGill University, Montreal, Canada. E-mail: chris.moraes@mcgill.ca*
[b] *Department of Surgery, McGill University Health Center, Montreal, Canada*
[c] *Department of Biological and Biomedical Engineering, McGill University, Montreal, Canada*
[d] *Goodman Cancer Research Center, McGill University, Montreal, Canada*

† Electronic supplementary information (ESI) available. See DOI: 10.1039/c7lc00356k

the bulk substrates into the cell culture solution, which influences biological function,[7,8] and the polymer matrix itself serves as a relatively infinite sink to sequester hydrophobic small molecules such as hormones and therapeutic candidates.[9] Hence, if these molecules are involved, experimental culture protocols that have been carefully and painstakingly developed on conventional plastic materials cannot be directly transferred to PDMS devices. This in turn makes it extremely challenging to interpret experimental results generated in PDMS devices compared to conventional culture systems, and could significantly interfere with bioassay results.

Alternative materials including thermoplastic polymers such as poly methyl methacrylate (PMMA), cyclic olefin copolymers (COC), polycarbonate (PC), polystyrene (PS), polyvinyl chloride (PVC), polyimide (PI), have been demonstrated as robust material platforms to generate disposable microfluidic devices.[19–22] In particularly, polystyrene is considered the gold standard for cell culture used in all Petri-dish type platforms, because it promotes cell attachment, does not sequester or leach molecules, is optically transparent for imaging purposes, and is compatible with high-volume manufacturing processes. Microfluidic devices constructed in polystyrene would therefore enable direct protocol transfer, and apples-to-apples comparisons with the established body of literature for a broad variety of biological systems.

Polystyrene devices can be fabricated *via* several techniques,[23–27] but these techniques each have significant limitations for academic research laboratories that require low volume prototyping and frequent design iterations. For example, hot embossing[28] and injection molding[29] are best suited for mass production of thermoplastic devices and have extremely high initial tooling costs, making iteration on designs a prohibitively expensive process. 3D printing and additive manufacturing technologies are also being developed for various materials,[30] but require significant initial investment in equipment, and relatively slow print-times for device production. The utility of these techniques are summarized in Table 1 in terms of their technical capabilities, cost comparison and quality of the finished part among others. More generally, each of these techniques requires specialized engineering knowledge and skill sets, making it even more challenging to produce devices on-site in a conventional biological research lab.

In this work, we present 'thermal scribing', an easily accessible rapid prototyping technique that can be used to make microfluidic devices in thermoplastic materials. This technique is based on using a heated 'pen' to locally heat thermoplastics to above the glass transition temperature in user-defined patterns. By placing the temperature-controlled tool in a commercially available and inexpensive desktop craft cutter, the tool can move along a defined path, carving micro channels directly on plastic substrates. By controlling the heat flux (through methods such as temperature variations, machining speeds, and proximity of the tool to the plastic) and the tool tip profile, a wide variety of microchannel configurations can be rapidly prototyped in plastic.

We demonstrate the practicality and utility of this technique by stimulating the formation of neutrophil extracellular traps (NETs) in a microfluidic channel. NET formation (NETosis)[31] occurs when neutrophils release their DNA into the extracellular environment, forming a protein web that can trap circulating bodies, and has been implicated in a wide variety of pathogenic and homeostatic disease processes.[32–35] While a few research groups have successfully initiated NETosis in PDMS microfluidic channels through stimulation with phorbyl 12-myristate 13-acetate (PMA),[36] PMA is a small hydrophobic molecule[37] that may be sequestered in the bulk PDMS, which could potentially affect NET formation and function. We compared PMA-activation of NETS in PDMS and polystyrene channels, and demonstrate that the presence of silicone rubbers significantly abrogates NET formation in human neutrophils, which therefore impacts the study of this phenomenon in conventional microfluidic systems.

2. Materials and methods

Unless otherwise stated, all cell culture materials and supplies were purchased from Fisher Scientific (Ottawa, ON), and chemicals from Sigma Aldrich (Oakville, ON).

Materials and fabrication

The protocol developed to fabricate thermally-scribed polystyrene microfluidic chips is outlined in Fig. 1. A commercially available desktop hobby craft cutter (KNK Zing; Klic-N-Kut; Apopka, FL, USA) costs ~$500 and was modified for thermal scribing by adding a soldering iron (Mudder 60 W iron) to the cutting head. To do so, a rubber stopper was cored to support and thermally isolate the soldering iron, placed directly into the craft cutter tool holder, and locked in place with a screw clamp. Replaceable soldering iron tool tips can be controlled between 200 and 400 °C, and selected based on desired channel cross-section. Control software (Make the

Table 1 Manufacturing capability and critical limitations of existing microfluidic fabrication techniques

	Existing microfluidic fabrication techniques					
	Soft lithography	Injection molding	Hot embossing	Laser machining	Micro milling	3D printing
Polystyrene fabrication	X	✓	✓	✓	✓	✓
Complex channel profiles	X	✓	✓	X	✓	✓
On-the-fly iterations	X	X	X	✓	✓	✓
Large area machining	✓	X	✓	✓	✓	X
Optical quality surface finish	✓	✓	✓	X	X	X
Basic start-up costs (<$10 000)	X	X	X	X	X	✓

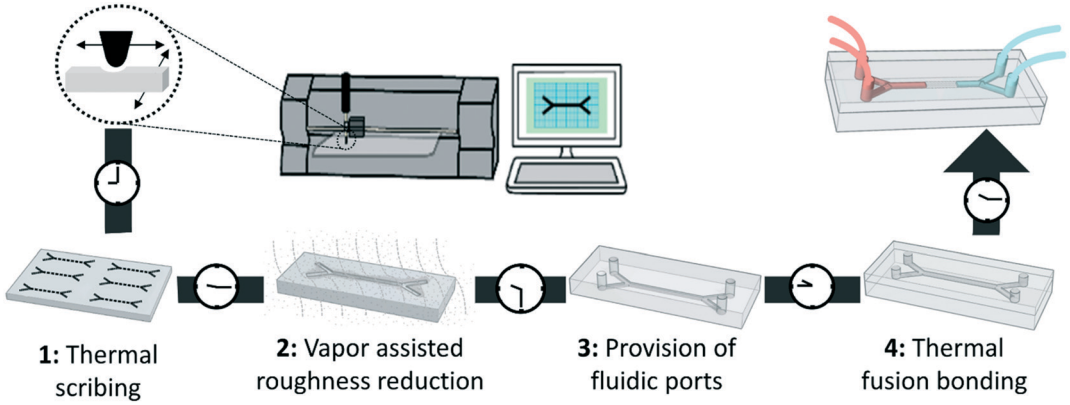

Fig. 1 Schematic illustration of the thermal scribing fabrication cycle with their typical time duration. The process involves using a hobbyist desktop craft cutter, modified with a soldering tool to thermally scribe CAD-designed channels into plastic materials. Surface roughness is then reduced using vapour phase acetone treatment, fluidic ports are created and fusion bonding is performed at elevated temperature to seal the device. Microfluidic devices can be produced in plastic materials within two hours of the CAD file being completed.

Cut; Muskego, WI) was then used to define the cutting speed, force and patterns generated as needed.

Surface machining

Polystyrene sheets (Plaskolite; Columbus, OH, USA) of 1 mm thickness were fed into the craft cutter and clamped under the cutters' cylindrical roller supports. The soldering iron was controlled at 200 °C for all described experiments. As the heated tool runs across the work part, the plastic material is locally melted in the heat-affected zone, creating channel features. For the structures reported in this work, an initial rough cut was used for bulk removal of material, and a second finishing cut at the same cutting speed was used to remove material debris. During this process, the re-flown plastic accumulates on either side of the channels and solidifies. These ridges are easily removed when cool by gently scraping the surface with a razor blade. Samples were then sonicated in a water bath at room temperature for 5 minutes, and dried under compressed air to remove any debris remaining from the machining process. Where applicable, surface roughness was reduced (ESI† Fig. S1) by vapour-phase solvent smoothing,[38] in which the device surfaces were exposed to a vapor of acetone and thereafter heated at a temperature below glass transition temperature. Clean polystyrene substrates were enclosed in a Petri dish with a paper towel soaked in acetone, sealed using a parafilm and placed in an oven at 70 °C for 20 minutes.

Device characterization

To study the cross-sectional channel parameters of the devices in detail, inverse replicas of the polystyrene microfluidic channels were cast in Sylgard 184 PDMS (Dow Corning). Briefly, a 10 : 1 mass ratio of pre-polymer to curing agent of was mixed, degassed, poured on the machined plastic surface and cured in a convection oven at 70 °C for 2 hours. The cured PDMS was easily peeled from the plastic surface, diced and imaged under the microscope. Results are reported as the average channel dimensions from two cross sections, for at least three separately fabricated channels.

Surface bonding and enclosed channel fabrication

Microstructured surfaces were sealed against flat polystyrene substrates using a simple thermal fusion bonding process,[39] in which the two polystyrene pieces were placed in contact, clamped between two glass slides, and heated in an oven for 30–60 minutes at slightly less than the glass transition temperature of the material (~100 °C).[40] Polymer chains diffuse between the mating surfaces of the softened plastic creating a strong fusion bond without altering chemical properties of the material. Connector tubes with 0.03″ inner diameter and 0.09″ outer diameter (EW-06419-03, Cole Parmer, Canada) were press fitted into the inlet/outlet ports and a layer of two part epoxy (LePage) was applied at the joint seal. Prior to any cell culture experiments, channels were rinsed with phosphate-buffered saline (PBS) and exposed to germicidal UV light for 5 minutes. For comparison purposes, fully PDMS channels were formed by replica molding (as outlined in the Device characterization section) and plasma-oxidation induced permanent bonding, following conventional protocols.[11] Hybrid PS–PDMS devices were prepared with thermally scribed microfluidic channels on PS substrates and weakly bonded to a PDMS substrate *via* plasma oxidation. All oxygen plasma treatments were performed in a PlasmaEtch chamber (2 minutes, 200 mTorr pressure, 20 ccm flow rate, and 60 W RF power). In addition to enabling substrate bonding, oxygen plasma treatment also enhanced cell adhesion on both PS and PDMS substrates.

Simulations and modelling

To study the evolution of the heat-affected zone during machining, finite element analysis (FEA) was carried out in COMSOL v.5.2a (Comsol Inc.; Burlington, MA, USA) by solving the heat conduction equation based on Fourier's law. A two-dimensional model was developed to simulate the tip of

the tool machining the plastic material at different cutting speeds. Although not perfectly accurate for tips with varying cross sectional geometries, such as a circle, this served as a first approximation for a tip passing over a plastic surface. One side of the two-dimensional domain was partitioned to include a fixed temperature boundary condition of 200 °C. The area of the work part was considered much larger than the size of the tool, to assign an insulation boundary condition for the plastic. The thermal conductivity and the heat capacity of the plastic material were taken as 0.033 W m^{-1} K^{-1} and 1400 J kg^{-1} K^{-1} respectively. Mesh sensitivity analysis and optimization was performed such that the coefficient of variation was <5%. The time evolution of the spatial temperature distribution in the plastic material was reported, and compared with experimentally-obtained channel profiles achieved using different cutting speeds.

Cell culture protocols

All cell culture experiments were performed in straight microfluidic channels with width 500 μm, height of 250 μm, and length 25 mm, fabricated in either polystyrene plastic or PDMS (using replica molding), and sealed against a polystyrene surface by fusion bonding, or PDMS surface by plasma oxidation. All incubations were conducted at 37 °C and 5% carbon dioxide. IMR-90 fetal lung fibroblasts (ATCC; stably transfected to express red fluorescent protein) were obtained as a gift from Dr. M. Park (McGill University), and sub-cultured according to manufacturer-prescribed protocols. Human neutrophils were isolated from the whole blood of healthy donors using a density gradient separation technique,[41] and stained with 1 μg mL^{-1} Ly6G-APC (e-bioscience). Neutrophils were introduced into the channels in a suspension of 10^6 cells per mL, while simultaneously being labelled with 5 μM sytox orange, with or without 500 nM phorbol 12-myristate 13-acetate (PMA) to stimulate the formation of extracellular traps, as per existing protocols.[36,41] Neutrophil NETosis was then assessed by fluorescent image analysis. To demonstrate the functional activity of the formed NETs, channels were then connected to a syringe pump, and unattached neutrophils were washed away under flow at 3.5 μL min^{-1} for 10 minutes. Murine Lewis lung carcinoma cell subline H59, transfected to express GFP[42] were maintained and sub-cultured in RPMI-1640 medium containing 10% FBS, 100 μg ml^{-1} penicillin, 100 μg ml^{-1} streptomycin, and 300 μg ml^{-1} glutamine; and flowed into the channels at 3.5 μL min^{-1} for 10 minutes to test cancer cell adhesion to the neutrophil extracellular traps.

Image analysis and statistics

Adhesion density was calculated as the number of adhered neutrophils per square millimeter of the microfluidic channel surface. The formation of neutrophil extracellular traps under various experimental conditions was quantified manually in ImageJ (NIH), in which the NETs ratio was calculated as the fraction of those neutrophils exhibiting classical NET morphology (extruded strands, flattened morphology). All comparisons were made using one- or two-way ANOVA analyses with Tukey post-hoc comparisons (SigmaStat; Systat Software, San Jose, CA), and graphical data is reported as means ± standard error for at least $n = 3$ independent experiments.

3. Results and discussion

Thermal scribing fabrication capabilities

The thermal scribing methodology presented here (Fig. 1) can be used to rapidly produce high-quality microfluidic channels in thermoplastic polymers. Fabrication can be conducted by users with minimal training and microfabrication expertise, and prototype devices in polystyrene can be produced within 90 minutes once a suitable CAD file is created. The craft cutter used here can handle a maximum width of 16 inch for the work part, useful for large area microfabrication, or creating multiple channels on the same work part ideally suited for low volume prototyping. In contrast, standard casting-based lithography techniques typically use 4–6 inch diameter wafers. The described thermal scribing fabrication equipment has the advantages of low setup costs, and excellent portability both within and between collaborating labs. Hence, in comparison with other fabrication techniques (Table 1), thermal scribing provides some unique advantages, particularly for rapid experimentation with conventional biological plastics.

To illustrate the utility of this strategy, we integrated polystyrene microfluidic channels into standard plastic well-plates (Fig. 2A), which would allow culture of cells on conventional surfaces, under microfluidically-controlled flow conditions while facilitating standard image-based analysis techniques. Fluorescent images were easily captured (Fig. 2B) and phase contrast bright field imaging was greatly improved through the described vapour-phase surface roughness reduction technique (Fig. S2†). Expected cell behaviour is observed in the PS microfluidic channels developed using the thermal scribing methodology, including spreading and proliferation as demonstrated with IMR90 fibroblasts over 24 hours of culture (Fig. 2B and S2†). We further demonstrate the ability to create single devices with gradually varying cross-sectional dimensions (Fig. 2C), which may have applications in parametrically manipulating applied fluid shear in such culture systems, and cannot be achieved using conventional single-layer photolithography-based fabrication strategies. Finally, we demonstrate that this technique can be applied to create substantially more advanced three-dimensional devices using multilayer construction strategies. Here, channels are scribed back-to-back on the same substrate, connected by vias and fusion-bonded as a stack (Fig. 2D), to create a 3D multilayer flow architecture.

Channel cross-section dimensions

Channel cross-section profiles play an important role in specialized microfluidic applications. For example, integrated nanovalves require rounded fluidic channels that can be completely sealed when a flexible membrane is pressurized, allowing control or actuation of flow.[43] Reasoning that heated tool tip profiles can be used to create channels with broadly

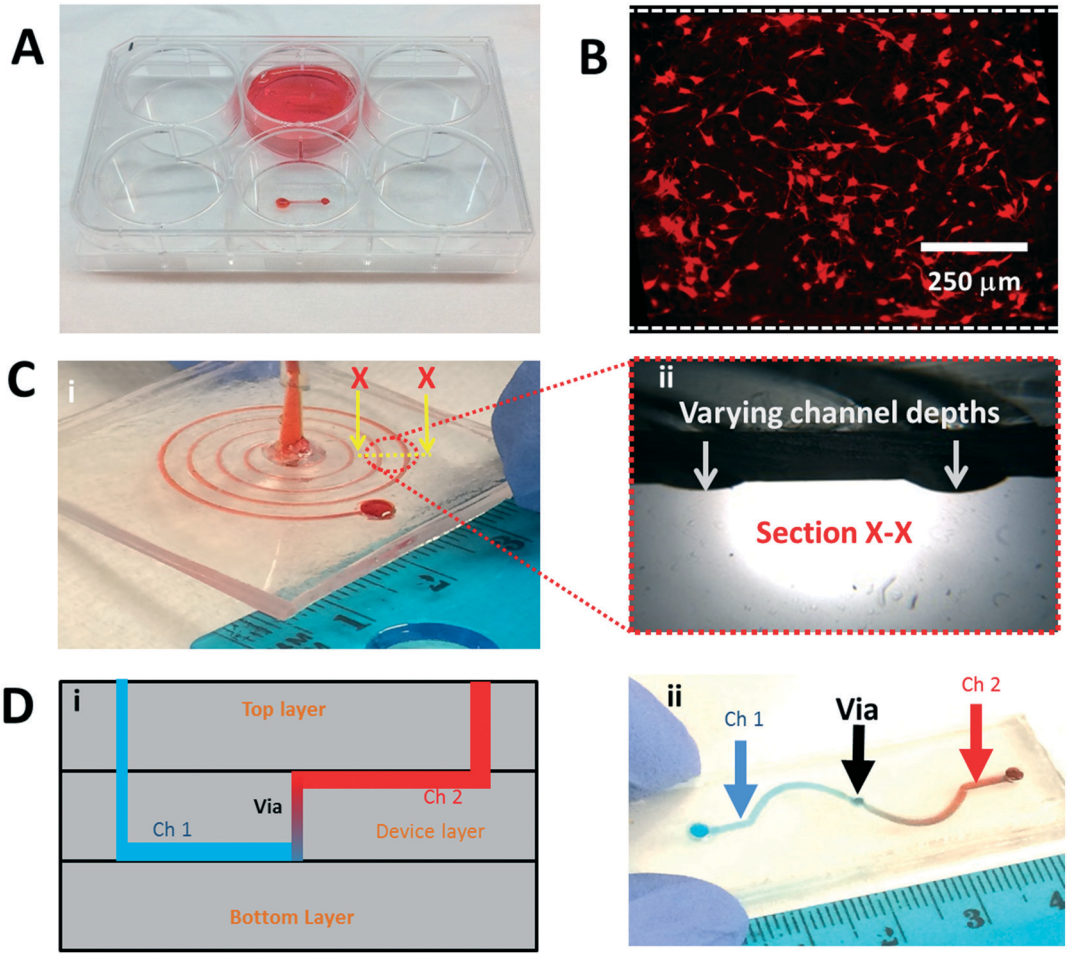

Fig. 2 Capabilities of the thermal scribing technique. (A) Polystyrene microfluidic channels can be integrated directly into standard biological culture plasticware, including 6-well plates. These systems allow (B) culture of fluorescently labeled IMR90 fibroblasts over 24 hours, demonstrating normal spreading and proliferation within thermally-scribed plastic microfluidic channels. More advanced structures can also be fabricated by thermal scribing including (C) a spiral microfluidic channel, with gradually varying cross-sectional dimensions (obtained using PDMS replica molding of the scribed channel); and (D) three-dimensional microfluidic devices formed by multilayer construction strategies. Channels (ch1 and ch2) are scribed back-to-back on the same substrate, connected by vias and fusion-bonded as a stack to create a multilayer flow architecture.

varying profiles, various tool tips were swapped in to create channels with triangular, rounded, flat-bottomed and trapezoidal cross-sections (Fig. 3), using the same process. Similar structures would be extremely challenging to fabricate using conventional photolithography techniques. Features that range in depth from 20 μm to 1 mm can be readily fabricated. Feature widths are dictated by the cutting tool available, but can be manipulated easily based on cutting speed and cutting force. Deep (low cutting speed) or shallow (high cutting speed) features can be formed using the same tool tip (Fig. 3). The global placement of features is limited by the craft cutter positioning resolution of 25 μm, which is more than sufficient for most polystyrene microfluidic layout applications.

Scribing process modeling

Channel features can be fabricated by manipulating a wide variety of parameters including cutting speed, cutting force, tool profile, and tool temperature. Hence, a process model is required to understand the relative impact of these parameters and obtain desired channel parameters on demand. We reasoned that channel profiles are dependent on (1) the mechanical abrasive force applied by the tool onto the surface; and (2) the heat transfer properties between machining tool and material, and the glass transition temperature of that material. We developed two process models to decouple these operational modes, each of which has distinct advantages.

To minimize any effects of heat transfer on channel dimensions, we set the tool height such that a physical stop limits the depth to which it can sink into the material, even under maximum applied cutting force. Under these conditions, a force threshold was established at 75% of the maximum cutting force (equivalent to ~560 gram-force), above which channels were reliably fabricated with consistent depths, regardless of cutting speed (Fig. 4A). Controlling the channel depth in this manner produces precise and repeatable results, but control over

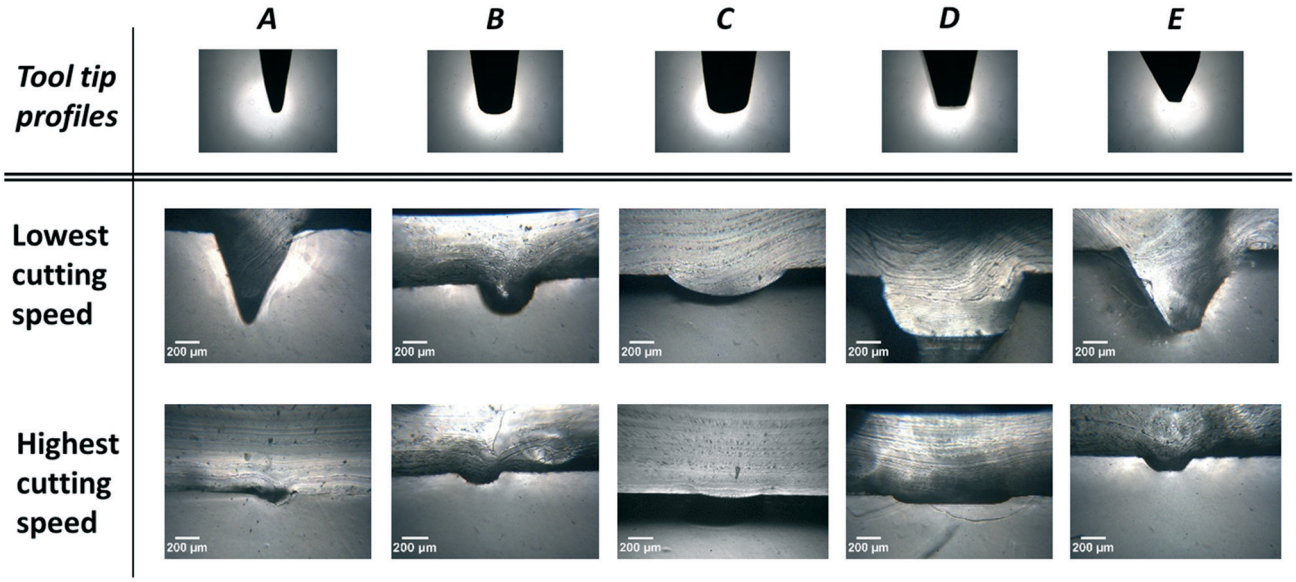

Fig. 3 Cross-sectional images of microfluidic channels obtained with different cutting tool tips. (A–E) show the cutting tool tip profiles that results in triangular, circular, curved, rectangular, and trapezoidal channel profiles respectively. The dimensions of the channels can be varied between 25 μm to 1 mm by adjusting the cutting speed.

absolute channel depth is dictated by manual positioning of the tool, which may vary in accuracy and depends on user skill.

Alternatively, varying cutting speed influences the total time for which the tool is in contact with a given point on the surface, which affects the total heat transferred from the tip of the tool to the plastic within that residence time. The time taken for the soldering iron to scribe one inch of plastic was measured for different speed settings, and the residence time associated with each cutting speed is the time taken by the tool tip to travel a distance equal to its width. Thus, for a given size of the tool tip, the temperature distribution in the plastic can be predicted by translating the cutting speeds to the residence time, using a finite element analysis. The tip of a flat-ended tool was modeled as a boundary on the plastic domain, with an associated temperature boundary condition (Fig. 4B). This simple model predicts a substantial variation in temperature profiles for different cutting speeds. The *x*- and *y*-spatial temperature distribution in the plastic material was then calculated for different cutting speeds (Fig. 4C). While the temperature variation along the *x*-axis is minimal for different residence times, there is a significant variation in the *y*-direction, suggesting that cutting time for a given tool tip primarily alters the depth of the carved channel, with only minimal impact on channel width. Comparing these simulation results with channel profiles obtained for different cutting speeds (Fig. 4D) showed strong agreement between model and experiment. Since channel geometry and profile can be controlled independently through tool selection and tuning the machining parameters appropriately, we provide a parametric look-up graph relating cutting tool width and cutting speed with expected channel width and depth (Fig. 4E) to fabricate custom devices.

NET formation is influenced by channel material

Cell-substrate adhesion simultaneously stimulates several adhesion receptors, which has been previously demonstrated to enhance NETosis.[44] Since culture substrate material plays a critical role in adhesion, we first confirmed that initial adhesion was not statistically distinct between PDMS and PS surfaces (Fig. 5A, $p = 0.121$), with or without PMA activation ($p > 0.05$, data not shown). These results indicate that adhesion differences do not select sub-populations of cells based on attachment, when compared to experiments on PDMS surfaces. When stimulated with 500 nM of PMA, NET activation was significantly enhanced on polystyrene devices (~65%) within 30 minutes, compared to hybrid devices (PDMS channels bonded to PS surfaces; ~35%, $p < 0.002$) or PDMS-only devices (~21%, $p < 0.001$; Fig. 5B). Since PMA is a reasonably small hydrophobic molecule,[37] we, like others,[36] believe it is being sequestered in PDMS and the reduced bioavailability of this activation agent decreases the fraction of neutrophils undergoing NETosis in microchannels fabricated partially or fully with PDMS. Finally, to confirm that the NETs formed in these devices are functionally active, a cancer cell capture assay was developed and performed (Fig. 5C). At high flow rates, NETs could be disrupted due to shear forces generated by flow, and hence all experiments were performed at low flow rates of ~3.5 μL min^{-1}. Cancer cells (labelled green) flowed over the NETs were selectively immobilized at the sites of NET formation in clustered patterns typical of this kind of assay conventionally done in macroscale flow chambers,[33] demonstrating that NETs formed in the polystyrene channels retain their functionality.

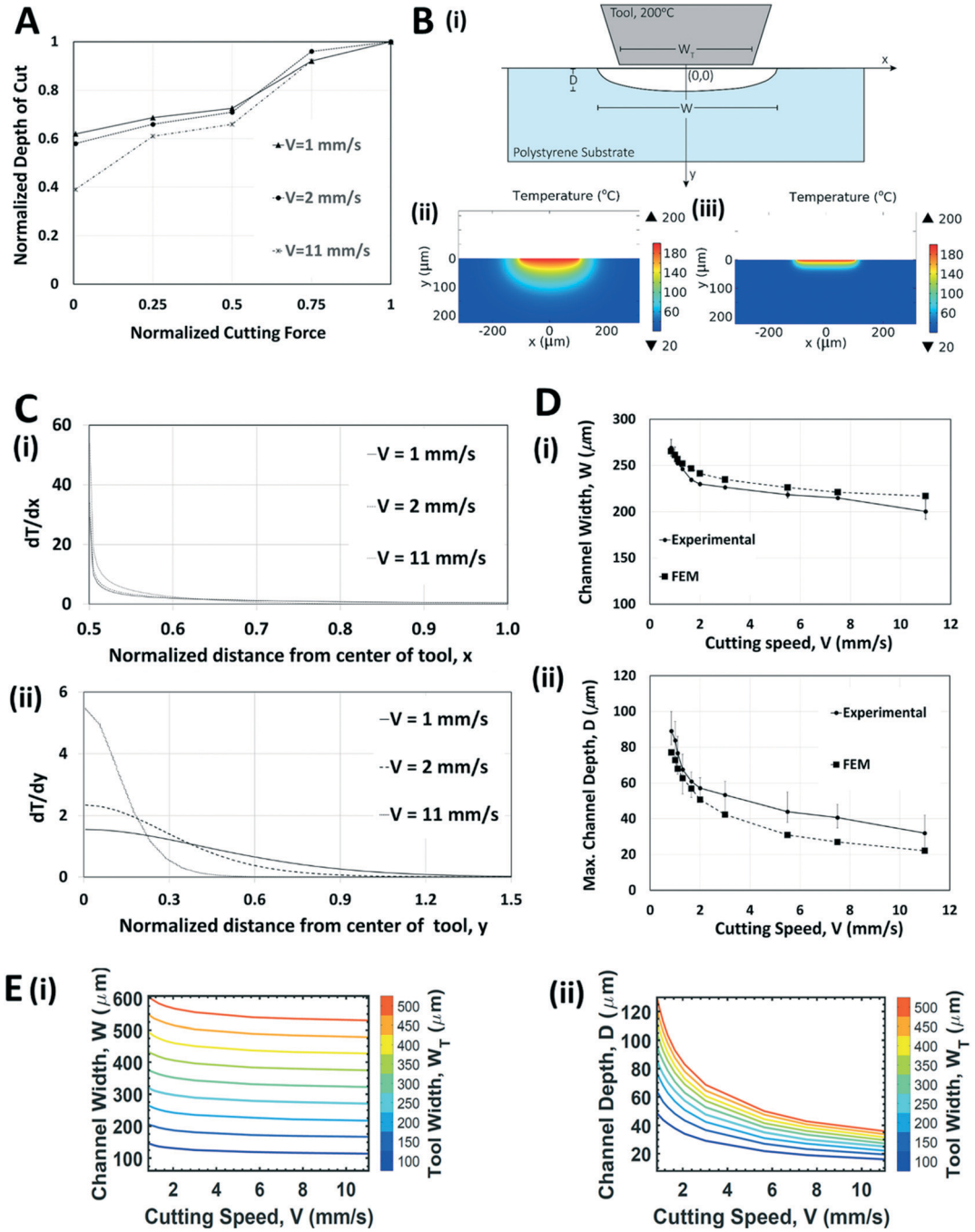

Fig. 4 Thermal scribing process modeling. (A) Experimental measurement of the effects of cutting force on the depth of cut in polystyrene (data presented as normalized to the depth obtained at maximum cutting force). When the maximum cutting force is reduced by 25%, the depth of cut varies by 8%. (B) Finite element models based on (i) geometry simulating a flat, 200 μm wide tool in contact with the surface were used to predict the distribution of heat in the polystyrene material at cutting speeds of (ii) 1 mm s^{-1} and (iii) 11 mm s^{-1}, demonstrating why increased cutting speed results in shallow channels. (C) Simulated variations in temperature from the edge of the tool tip along the (i) *x* and (ii) *y* axes based on different cutting speeds suggests that cutting speed primarily alters channel depth, while maintaining channel width. (D) When compared with experimental results for (i) cut width and (ii) cut depth, the finite element simulations adequately predict channel dimensions (n = 3, mean ± SEM). (E) The developed models were applied to predict (i) widths and (ii) depths of the microfluidic channels obtained for different tool sizes (100–500 μm) at various cutting speeds.

Discussion

Quantifying the percentage of NET release in culture is often used as a surrogate metric for NET quality.[45] It has previously been established that only ~30–40% of neutrophils in culture produce NETs when stimulated with 500 nM of PMA.[33,36] In PDMS-based microfluidic devices, ~40% of neutrophils undergo NETosis under PMA stimulation even when treated for several

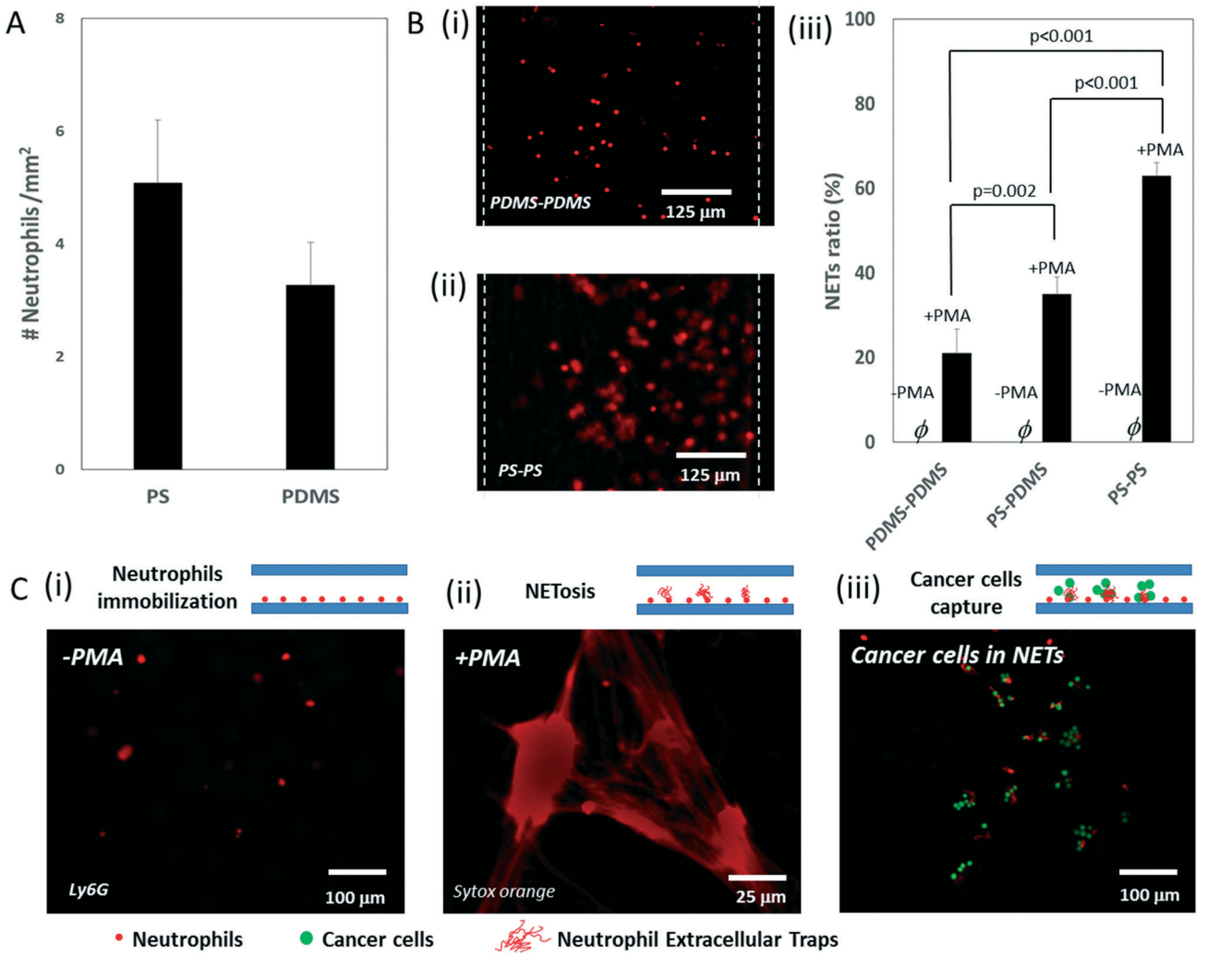

Fig. 5 Application of plastic microfluidic channels to create functional neutrophil extracellular traps by stimulation with PMA. (A) Initial neutrophil adhesion to polystyrene and PDMS surfaces are not statistically different (p = 0.121). (B) When stimulated with PMA, neutrophils in (i) PDMS or hybrid PS–PDMS channels exhibited low levels of NET activation, while (ii) a significant fraction of neutrophils in polystyrene-only devices underwent NETosis. (iii) Quantitative comparison of NETosis levels based on morphological analysis in silicone *vs.* plastic channels (n = 3, mean ± SEM). No NETosis was observed without PMA stimulation. (C) To confirm that the microfluidically-formed NETs are functional, a simple cancer cell capture assay was developed. (i) Neutrophils are first allowed to adhere onto the channel surface. (ii) The neutrophils are stimulated with PMA to form characteristic NET structures, and (iii) murine lung carcinoma cells (labelled green), are found to attach selectively to regions where NETs have been initiated.

hours,[36] matching our experimental observations for NETosis in hybrid PDMS–PS channels. Although the underlying reasons for this increase remain unknown, it may be due to elevated autocrine signaling concentration in confined microfluidic channels. Interestingly, we observe a significant increase in NETosis in polystyrene microfluidic channels (~65%) than is ordinarily seen under stimulation with 500 nM or more of PMA. We believe that this effect may be caused by the sequestration of hydrophobic PMA molecules by PDMS, given the well-known ability of PDMS to absorb small hydrophobic molecules such as estrogen.[9,17] This further suggests that the original macroscale flow experiments may have been influenced by the presence of silicone rubber, often used in connective tubing or as a gasket in parallel plate flow chambers. The higher NETs fraction observed with polystyrene microfluidic channels may hence be more representative of *in vivo* neutrophil NETosis, and this work thus provides further evidence that use of PDMS materials significantly impacts biological outcomes in microfabricated devices.

More broadly, the described thermal scribing technique offers considerable benefits for researchers interested in using thermoplastics for biomicrofluidic device development. The initial setup (<$1k) and production costs (<$2 per device) present low barriers to adoption, and the setup can be readily re-tooled and repositioned within minutes to easily specify the required channel dimensions and channel profiles. Furthermore, bonding and sealing devices, typically a weak-point in elastomeric device fabrication, is reliable and does not require expensive plasma-cleaning equipment. The simple solvent exposure technique that was developed to reduce surface roughness (Fig. S1†) is applicable to a range of

different plastics manufactured by different methods. Several devices of different design contours can be fabricated on the same plastic sheet, which is ideal for rapid low volume fabrication. Finally, the data presented demonstrates the need to carefully consider the device fabrication material, particularly at the experimental prototyping stage, to ensure robust and realistic function for certain biological systems.

4. Conclusion

In this work, we have developed a simple and accessible rapid prototyping technique using a hobbyist benchtop craft cutter and a temperature controlled soldering tool, to develop microfluidic devices on thermoplastics. The thermal scribing technique proves to be a highly cost effective alternative to fabricating microfluidic channels directly on plastics, compared to conventional plastic machining techniques. The synthesis of plastic based microfluidic channels through this simple prototyping process simplifies the process of integrating microfluidics into existing plastic based culture platforms such as multiwall plates and culture dishes, enabling direct transfer of experimental protocols and comparison between macroscale culture controls.

Acknowledgements

The authors would like to thank Mr. Phil Vourtzoumis for assistance with neutrophil isolation, Mr. Jack Mouhanna for his assistance with confocal imaging, and Ms. Jessica Ronci for early experimentation with the craft cutter. This project has been supported by the American Association of Thoracic Surgeon's Graham Foundation and the McGill University Health Center Research Institute to JS; and the Natural Sciences and Engineering Research Council of Canada, and the Canada Research Chairs program to CM.

References

1 M. Karimi, S. Bahrami, H. Mirshekari, S. M. M. Basri, A. B. Nik, A. R. Aref, M. Akbari and M. R. Hamblin, Microfluidic systems for stem cell-based neural tissue engineering, *Lab Chip*, 2016, **16**(14), 2551–2571.

2 H. Yin and D. Marshall, Microfluidics for single cell analysis, *Curr. Opin. Biotechnol.*, 2012, **23**(1), 110–119.

3 J. R. Heath, A. Ribas and P. S. Mischel, Single-cell analysis tools for drug discovery and development, *Nat. Rev. Drug Discovery*, 2016, **15**(3), 204–216.

4 A. Chandresekaran, M. Abduljawad and C. Moraes, Have Microfluidics Delivered for Drug Discovery?, *Expert Opin. Drug Discovery*, 2016, **11**(8), 745–748.

5 M. S. Ferry, I. A. Razinkov and J. Hasty, Microfluidics for synthetic biology: from design to execution, *Methods Enzymol.*, 2011, **497**, 295.

6 A. H. Ng and A. R. Wheeler, Next-Generation Microfluidic Point-of-Care Diagnostics, *Clin. Chem.*, 2015, **61**(10), 1233–1234.

7 K. J. Regehr, M. Domenech, J. T. Koepsel, K. C. Carver, S. J. Ellison-Zelski, W. L. Murphy, L. A. Schuler, E. T. Alarid and D. J. Beebe, Biological implications of polydimethylsiloxane-based microfluidic cell culture, *Lab Chip*, 2009, **9**(15), 2132–2139.

8 S. Halldorsson, E. Lucumi, R. Gómez-Sjöberg and R. M. Fleming, Advantages and challenges of microfluidic cell culture in polydimethylsiloxane devices, *Biosens. Bioelectron.*, 2015, **63**, 218–231.

9 B. J. van Meer, H. de Vries, K. S. A. Firth, J. van Weerd, L. G. J. Tertoolen, H. B. J. Karperien, P. Jonkheijm, C. Denning, A. P. IJzerman and C. L. Mummery, Small molecule absorption by PDMS in the context of drug response bioassays, *Biochem. Biophys. Res. Commun.*, 2016, **482**(2), 323–328.

10 C. W. Tsao, Polymer Microfluidics: Simple, Low-Cost Fabrication Process Bridging Academic Lab Research to Commercialized Production, *Micromachines*, 2016, **7**(12), 225.

11 J. C. McDonald and G. M. Whitesides, Poly (dimethylsiloxane) as a material for fabricating microfluidic devices, *Acc. Chem. Res.*, 2002, **35**(7), 491–499.

12 S. Cosson, L. G. Aeberli, N. Brandenberg and M. P. Lutolf, Ultra-rapid prototyping of flexible, multi-layered microfluidic devices via razor writing, *Lab Chip*, 2015, **15**(1), 72–76.

13 M. Islam, R. Natu and R. Martinez-Duarte, A study on the limits and advantages of using a desktop cutter plotter to fabricate microfluidic networks, *Microfluid. Nanofluid.*, 2015, **19**(4), 973–985.

14 J. Do, J. Y. Zhang and C. M. Klapperich, Maskless writing of microfluidics: Rapid prototyping of 3D microfluidics using scratch on a polymer substrate, *Robot. Comput. Integr. Manuf.*, 2011, **27**(2), 245–248.

15 B. C. Kim, C. Moraes, J. Huang, M. D. Thouless and S. Takayama, Fracture-based micro-and nanofabrication for biological applications, *Biomater. Sci.*, 2014, **2**(3), 288–296.

16 B. C. Kim, T. Matsuoka, C. Moraes, J. Huang, M. D. Thouless and S. Takayama, Guided fracture of films on soft substrates to create micro/nano-feature arrays with controlled periodicity, *Sci. Rep.*, 2013, **3**, 3027.

17 E. Berthier, E. W. Young and D. Beebe, Engineers are from PDMS-land, Biologists are from Polystyrenia, *Lab Chip*, 2012, **12**(7), 1224–1237.

18 J. Zhou, A. V. Ellis and N. H. Voelcker, Recent developments in PDMS surface modification for microfluidic devices, *Electrophoresis*, 2010, **31**(1), 2–16.

19 K. Liu and Z. H. Fan, Thermoplastic microfluidic devices and their applications in protein and DNA analysis, *Analyst*, 2011, **136**(7), 1288–1297.

20 A. Bhattacharyya and C. M. Klapperich, Thermoplastic microfluidic device for on-chip purification of nucleic acids for disposable diagnostics, *Anal. Chem.*, 2006, **78**(3), 788–792.

21 D. Konstantinou, A. Shirazi, A. Sadri and E. W. Young, Combined hot embossing and milling for medium volume production of thermoplastic microfluidic devices, *Sens. Actuators, B*, 2016, **234**, 209–221.

22 A. M. Wan, A. Sadri and E. W. Young, Liquid phase solvent bonding of plastic microfluidic devices assisted by retention grooves, *Lab Chip*, 2015, **15**(18), 3785–3792.

23 R. Tran, B. Ahn, D. R. Myers, Y. Qiu, Y. Sakurai, R. Moot, E. Mihevc, H. T. Spencer, C. Doering and W. A. Lam, Simplified prototyping of perfusable polystyrene microfluidics, *Biomicrofluidics*, 2014, **8**(4), 046501.

24 R. Peng and D. Li, Fabrication of nanochannels on polystyrene surface, *Biomicrofluidics*, 2015, **9**(2), 024117.

25 H. Li, Y. Fan, R. Kodzius and I. G. Foulds, Fabrication of polystyrene microfluidic devices using a pulsed CO2 laser system, *Microsyst. Technol.*, 2012, **18**(3), 373–379.

26 R. Suriano, A. Kuznetsov, S. M. Eaton, R. Kiyan, G. Cerullo, R. Osellame, B. N. Chichkov, M. Levi and S. Turri, Femtosecond laser ablation of polymeric substrates for the fabrication of microfluidic channels, *Appl. Surf. Sci.*, 2011, **257**(14), 6243–6250.

27 D. J. Guckenberger, T. E. de Groot, A. M. Wan, D. J. Beebe and E. W. Young, Micromilling: a method for ultra-rapid prototyping of plastic microfluidic devices, *Lab Chip*, 2015, **15**(11), 2364–2378.

28 E. W. Young, E. Berthier, D. J. Guckenberger, E. Sackmann, C. Lamers, I. Meyvantsson, A. Huttenlocher and D. J. Beebe, Rapid prototyping of arrayed microfluidic systems in polystyrene for cell-based assays, *Anal. Chem.*, 2011, **83**(4), 1408–1417.

29 M. Heckele and W. K. Schomburg, Review on micro molding of thermoplastic polymers, *J. Micromech. Microeng.*, 2003, **14**(3), R1.

30 N. Bhattacharjee, A. Urrios, S. Kang and A. Folch, The upcoming 3D-printing revolution in microfluidics, *Lab Chip*, 2016, **16**(10), 1720–1742.

31 V. Brinkmann, U. Reichard, C. Goosmann, B. Fauler, Y. Uhlemann, D. S. Weiss, Y. Weinrauch and A. Zychlinsky, Neutrophil extracellular traps kill bacteria, *Science*, 2004, **303**(5663), 1532–1535.

32 J. J. Cools-Lartigue, J. D. Spicer, B. McDonald, S. Chow, P. Kubes and L. E. Ferri, Neutrophil extracellular traps sequester circulating tumor cells in vitro and in a murine model of metastasis, *Cancer Res.*, 2012, **72**(8 Supplement), 2972.

33 T. A. Fuchs, U. Abed, C. Goosmann, R. Hurwitz, I. Schulze, V. Wahn, Y. Weinrauch, V. Brinkmann and A. Zychlinsky, Novel cell death program leads to neutrophil extracellular traps, *J. Cell Biol.*, 2007, **176**(2), 231–241.

34 F. H. Pilsczek, D. Salina, K. K. Poon, C. Fahey, B. G. Yipp, C. D. Sibley, S. M. Robbins, F. H. Green, M. G. Surette, M. Sugai and M. G. Bowden, A novel mechanism of rapid nuclear neutrophil extracellular trap formation in response to *Staphylococcus aureus*, *J. Immunol.*, 2010, **185**(12), 7413–7425.

35 J. Cools-Lartigue, J. Spicer, B. McDonald, S. Gowing, S. Chow, B. Giannias, F. Bourdeau, P. Kubes and L. Ferri, Neutrophil extracellular traps sequester circulating tumor cells and promote metastasis, *J. Clin. Invest.*, 2013, **123**(8), 3446–3458.

36 S. F. Moussavi-Harami, K. M. Mladinich, E. K. Sackmann, M. A. Shelef, T. W. Starnes, D. J. Guckenberger, A. Huttenlocher and D. J. Beebe, Microfluidic device for simultaneous analysis of neutrophil extracellular traps and production of reactive oxygen species, *Integr. Biol.*, 2016, **8**(2), 243–252.

37 D. PaDma and K. M. Bhat, A Comparison Between Phorbol 12 Myristate 13 Acetate and Phorbol 12, 13 Dibutyrate in Human Melanocyte Culture, *J. Clin. Diagn. Res.*, 2016, **10**(1), GC01.

38 I. R. G. Ogilvie, V. J. Sieben, C. F. A. Floquet, R. Zmijan, M. C. Mowlem and H. Morgan, Reduction of surface roughness for optical quality microfluidic devices in PMMA and COC, *J. Micromech. Microeng.*, 2010, **20**(6), 065016.

39 C. W. Tsao and D. L. DeVoe, Bonding of thermoplastic polymer microfluidics, *Microfluid. Nanofluid.*, 2009, **6**(1), 1–16.

40 J. Rieger, The glass transition temperature of polystyrene: results of a round robin test, *J. Therm. Anal. Calorim.*, 1996, **46**(3–4), 965–972.

41 S. Najmeh, J. Cools-Lartigue, B. Giannias, J. Spicer and L. E. Ferri, Simplified Human Neutrophil Extracellular Traps (NETs) Isolation and Handling, *J. Visualized Exp.*, 2015(98), e52687.

42 P. Auguste, L. Fallavollita, N. Wang, J. Burnier, A. Bikfalvi and P. Brodt, The host inflammatory response promotes liver metastasis by increasing tumor cell arrest and extravasation, *Am. J. Pathol.*, 2007, **170**, 1781–1792.

43 M. A. Unger, H. P. Chou, T. Thorsen, A. Scherer and S. R. Quake, Monolithic microfabricated valves and pumps by multilayer soft lithography, *Science*, 2000, **288**(5463), 113–116.

44 V. Brinkmann and A. Zychlinsky, Beneficial suicide: why neutrophils die to make NETs, *Nat. Rev. Microbiol.*, 2007, **5**(8), 577–582.

45 N. de Buhr and M. von Köckritz-Blickwede, How Neutrophil Extracellular Traps Become Visible, *J. Immunol. Res.*, 2016, 4604713.

